

In Situ NMR Studies of the Conversion of Methanol into Gasoline on Aluminosilicate and Gallosilicate Offretites

María D. Alba,^{†,‡} Antonio A. Romero,^{†,§} Mario L. Occelli,^{||} and Jacek Klinowski*,[†]

Department of Chemistry, University of Cambridge, Lensfield Road, Cambridge CB2 1EW, U.K., and Zeolite and Clay Program, Georgia Tech Research Institute, Georgia Institute of Technology, Atlanta, Georgia 30332

Received: January 6, 1997; In Final Form: April 24, 1997[®]

The conversion of CH₃OH by the hydrogen forms of three offretites with different contents of framework Al and Ga has been monitored by ¹³C NMR with magic-angle spinning. At 150 °C methanol is dehydrated to dimethyl ether. No hydrocarbons are produced below 300 °C, and the equilibrium product distribution is achieved only at 370 °C. The distribution of both the intermediates and the final products is different for each of the three catalysts. Thus, branched long-chain hydrocarbons form in the intracrystalline space of Ga-offretite but not in Al,Ga- and Al-offretites. More methane is formed over the aluminum-containing samples, ca. 3.2% in Al-offretite and ca. 3.7% in Al,Ga-offretite, than in Ga-offretite (ca. 2.0%). No appreciable amount of aromatic species is detected at any temperature. We believe that the methanol-to-gasoline process over Al,Ga-offretites is bifunctional and involves Brønsted acid sites as well as extraframework Ga species.

Introduction

Isomorphous substitution of silicon in zeolitic frameworks by trivalent elements such as Ga,^{1,2} Al,^{3,4} and B⁵ modifies the acid properties of the catalysts.^{6–8} In particular, [Si,Ga]-analogues of zeolite ZMS-5 exhibit a catalytic activity for cracking of hydrocarbons that is similar to that of [Si,Al]-ZSM-5.^{9,10} Gallium-containing zeolitic catalysts are thought to be bifunctional^{10–12} with conversion involving Brønsted protons associated with four-coordinate Ga in “bridging” Ga–OH–Si sites and six-coordinate (extraframework) gallium.

As the important first step in the methanol-to-gasoline (MTG) process,¹³ the adsorption of methanol in zeolites has been the subject of many experimental^{13–17} and theoretical^{18–22} studies. Considerable effort was devoted to the clarification of the nature of the various reactions involved. Shape selectivity has also attracted much attention,^{23–26} and the precise mechanism of the formation of the first C–C bond, whereby dimethyl ether (DME) formed by dehydration of methanol (MeOH) is transformed into C₂ hydrocarbons such as ethylene, is the most important single issue that remains unresolved. An understanding of these processes at the molecular level will ultimately lead to the design of catalysts with improved efficiency, specificity, and selectivity.

The application of spectroscopic methods is an important area in catalysis.²⁷ Over the past decade or so it has become clear that the nature and chemical status of the species generated in the intracrystalline space of molecular sieves in the course of catalytic reactions can be successfully studied in situ using ¹³C magic-angle-spinning (MAS) NMR.^{14,15,28–33} We have applied in situ ¹³C MAS NMR^{14,29} to study the conversion of MeOH over offretite in which gallium or/and aluminum were isomorphously substituted for silicon. The cages of offretite are connected through unrestricted 12-membered ring apertures

forming parallel channels ca. 6.3 Å in diameter, which span the entire length of the crystal in the *c* direction.^{34–36} As a result, offretite adsorbs organic molecules of up to 6.0 Å in diameter.

We are fully aware that the conditions inside a sealed glass microreactor are not the same as those in the flow system that is actually used in industrial applications. Furthermore, given the experimental procedure, the precise pressure inside the microreactor is not accurately known and may vary as the reaction proceeds. Unfortunately, alternative procedures, such as magic-angle spinning using ¹³C-enriched spinning gas, are totally impracticable in view of the enormous cost involved. Despite these reservations, we submit that the technique used in this work allows us to monitor in situ the evolution of the various products and intermediates in the MTG process, leading to information that is unavailable to other methods, such as gas chromatography (in view of the differential adsorption of the various species and their different diffusional properties).

Experimental Section

Preparation of Samples. Molecular sieves with the offretite structure have been synthesized from hydrogels of composition 1.0M₂O₃:12SiO₂:1.5Na₂O:2.2K₂O:4.0(TMA)₂O:250H₂O where M = Al or Ga and TMA stands for tetramethylammonium from tetramethylammonium chloride. The required Al/Ga ratio of the gel was obtained by adding a clear aqueous solution of sodium gallate. Crystallization proceeded (without stirring) in Teflon-lined Berghoff autoclaves heated at 95 °C for 48 h. The product was washed with distilled water, dried at 100 °C in an air oven, calcined in air at 550 °C for 10 h in order to remove the organic template, and stored under ambient conditions. Powder X-ray diffraction (XRD) showed that all samples were highly crystalline. Ammonium-exchanged forms of offretite were prepared by repeated treatment of the crystals with a 2 M aqueous solution of NH₄NO₃ at 60 °C, and the hydrogen forms were made by heating the ammonium-exchanged forms at 500 °C for 4 h in flowing air.³⁷ XRD, nitrogen adsorption/desorption

[†] University of Cambridge.

[‡] On leave from Departamento de Química Inorgánica, Instituto Ciencia de los Materiales, Universidad de Sevilla, C.S.I.C., P.O. Box 874, 41012 Sevilla, Spain.

[§] On leave from Departamento de Química Orgánica, Universidad de Córdoba, San Alverto Magno s/n, 14004 Córdoba, Spain.

^{||} Georgia Institute of Technology.

[®] Abstract published in *Advance ACS Abstracts*, June 1, 1997.

TABLE 1: Oxide Composition (Mole Ratios) of the Samples of Offretite after Ion Exchange and Calcination^a

	Al ₂ O ₃	Ga ₂ O ₃	SiO ₂	Na ₂ O	K ₂ O
Ga-offretite		1.00	7.65	0.030	
Al,Ga-offretite	0.85	0.15	7.71	0.001	0.09
Al-offretite	1.00		7.79	0.033	0.17

^a Estimated accuracy is $\pm 5\%$ of each value.

TABLE 2: Sample Characterization^a

	unit cell parameter <i>a</i> (Å)	sorptive properties	
		<i>S_μ</i> (m ² g ⁻¹)	<i>V_μ</i> (cm ³ g ⁻¹)
Ga-offretite	12.9	220.06	0.104
Al,Ga-offretite	13.0	359.64	0.167
Ga-offretite	13.2	434.39	0.203

^a *S_μ* is the micropore area and *V_μ* the micropore volume. Estimated accuracy is 0.05 Å for unit cell parameters and $\pm 5\%$ for *S_μ* and *V_μ*.

isotherms, and ²⁹Si, ²⁷Al, and ⁷¹Ga MAS NMR (results not shown) all indicate a decrease of sample crystallinity as a result of calcination. Some six-coordinate (extraframework) Al and Ga are generated during calcination, and the subsequent removal of extraframework Ga is easier than the removal of Al. Microcalorimetry with ammonia as a probe molecule indicates that the insertion of gallium into the aluminosilicate framework results in a heterogeneity of the acid sites: Brønsted acidity decreases while Lewis acidity increases. The bulk compositions of the three samples of offretite are given in Table 1 and their sorptive properties in Table 2.

Nitrogen sorption isotherms for all three offretites are of type I, typical of microporous materials. Although widely used for the assessment of microporosity,³⁸ the simple measurement of the surface area, total adsorbed volume, or pore size distribution can give a misleading picture of the accessible volume. By contrast, the “*t*-plot” method estimates microporosity by comparing the shape of an isotherm with that for a standard nonporous solid. The microporous volume is then determined from the intercept of the linear trace extrapolated to the *y*-axis, and the external surface is calculated from the slope.

For MAS NMR measurements, a small quantity (ca. 200 mg) of each catalyst was placed in a Pyrex capsule designed to fit inside a zirconia MAS rotor³⁹ and the capsule connected to a vacuum line. The catalyst was activated by heating at 400 °C for 6 h under vacuum, equilibrated with an overpressure of 50 Torr of 30 wt % ¹³C-enriched CH₃OH at 20 °C, and allowed to equilibrate for 1 h before being isolated from the bulk of the gaseous MeOH. The capsule was sealed off under liquid nitrogen to prevent the onset of catalytic processes. The capsule could then be heated to the desired reaction temperature for various lengths of time, quenched, and placed in the NMR rotor to record ¹³C NMR spectra at ambient temperature.

NMR Spectra. All spectra were recorded on a Chemagnetics CMX-400 spectrometer with zirconia rotors 7.5 mm in diameter, spun in nitrogen gas at rates of up to 2 kHz. To make them quantitatively reliable, the ¹³C MAS spectra were recorded with high-power decoupling but without cross-polarization (CP). ¹H–¹³C CP/MAS NMR spectra and dipolar-dephased spectra were measured only to establish whether protons are attached to a given carbon atom and to distinguish between mobile and immobile species. High-power proton decoupling experiments were carried out with 45° ¹³C pulses with a repetition time of 10 s and 300 scans. The longest ¹³C *T*₁ relaxation time is approximately 1.5 s so that a 10 s recycle time is sufficient to provide quantitatively reliable spectra. Experiments without high-power decoupling used the same acquisition parameters. Cross-polarization spectra were acquired with a 7.3 μs proton

TABLE 3: Assignment of ¹³C MAS NMR Lines in the Aliphatic Region (10–40 ppm) in Figures 1–3 and 5 for Samples Treated at 300 and 370 °C

aliphatic compounds	peak number	300 °C, 11 h			370 °C, 10 h		
		Ga-	Al,Ga-	Al-	Ga-	Al,Ga-	Al-
methane	21	m	s	s	m	m	m
ethane	19	w	vw	w	w	vw	w
propane	13			w		vw	m
butane	9, 14	m	m	m	m	m	m
<i>n</i> -pentane	4, 10, 14	m	m		vw	w	w
<i>n</i> -hexane	5, 10, 14	m	m	vw	w	w	w
<i>n</i> -heptane	5, 6, 10, 14	m	m	w	w	m	m
isobutane	9	s	s	s	m	m	m
isopentane	5, 6, 11, 15	m	m	s	m	m	m
isohexane	12, 16	m	m	m	m	m	m
neopentane	5, 7	vw	vw	w	vw	—	vw
neohexane	3, 5, 6, 17	w	vw	vw	vw	vw	vw
3-methylpentane	1, 5, 11, 16	m	w	m	m	m	m
2,3-dimethylbutane	1, 11	vw		m	m	m	m
3,3-dimethylpentane	3, 8, 18	vw					m
cyclopropane	20			w	vw		

^a The meaning of the abbreviated descriptions of peak intensity: s = strong, m = medium, w = weak, and vw = very weak.

90° pulse, a 4 ms contact time, and a 4 s repetition time. Dipolar-dephased spectra were acquired under the same conditions as the cross-polarization spectra, using dephasing times of 60, 100, 200, and 500 μs. Chemical shifts are given in ppm from external tetramethylsilane (TMS).

Results

The ¹³C MAS NMR spectra of all three offretites with 50 Torr of adsorbed MeOH and maintained at 20 °C each contain a single resonance at 50.8 ppm from the methyl carbon of the adsorbed MeOH.⁴⁰ After the samples were heated at 150 °C, two new lines appear, at 60.5 and 57.0 ppm, corresponding to adsorbed and gaseous DME, respectively. Further heating to 250 °C for 3 h does not produce carbon monoxide, as it does in zeolite H-ZSM-5,^{14,29} or any aliphatic compounds.

The catalysts were next heated at 300 °C for increasing periods of time and examined after each thermal treatment. Figures 1–3 show the ¹³C NMR spectra of Ga-offretite, Al,Ga-offretite, and Al-offretite, respectively, recorded with proton decoupling only. The assignment of the various spectral features (Table 3) was done by reference to the published chemical shift data,⁴¹ taking into account the likelihood of a small susceptibility shift for aliphatic molecules in the adsorbed phase, which for saturated hydrocarbons in zeolites is never greater than 1.5 ppm.⁴² Although some resonances overlap, all could be reliably assigned because most compounds give rise to several NMR peaks. We have assigned the two peaks with negative chemical shifts (−6.1 and −10.7 ppm) to gaseous cyclopropane and methane^{14,29} for the following reason. In their study of the MTG process over silicoaluminophosphate molecular sieve SAPO-34, Xu et al.⁴³ assigned lines at −7 and −11 ppm to methane in two different chemical environments because when recorded with no proton decoupling, both spectral lines were split into two quintets with *J*_{C–H} ≈ 125 Hz, characteristic of methane. However, in our spectra recorded without decoupling, the line at −11 ppm was indeed split into a quintuplet with *J*_{C–H} ≈ 125 Hz, but the line at −7 ppm became broad but unsplit. This led us to assign the line at −7 ppm to cyclopropane, as in the case of a ZSM-5 catalyst^{14,29} and not to methane in a different environment, as for SAPO-34.⁴³

Relative concentrations of the various species present in the catalyst samples were determined by integrating the deconvol-

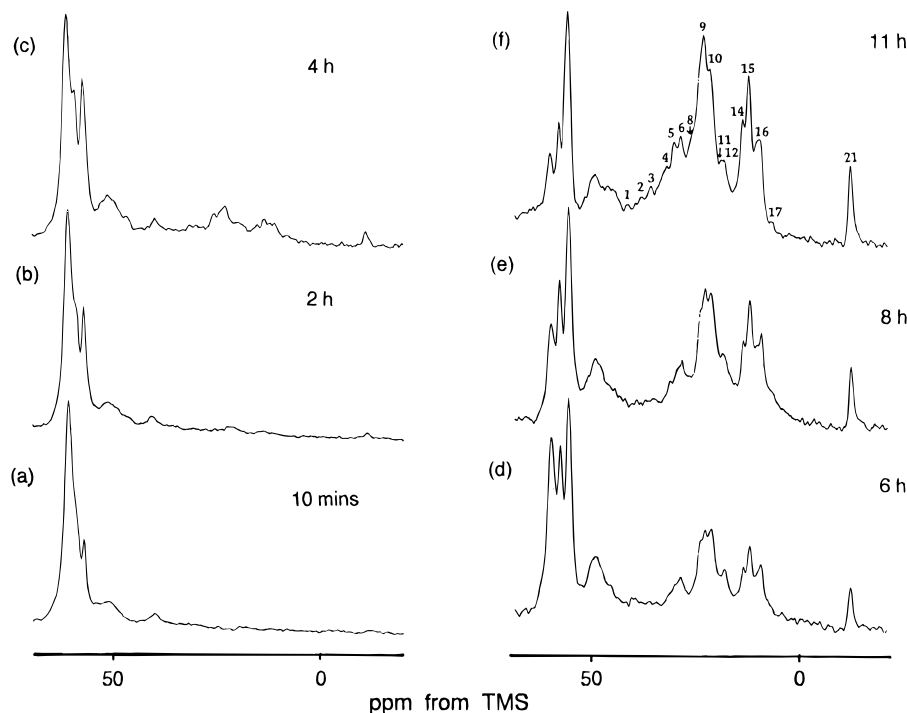
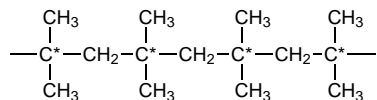
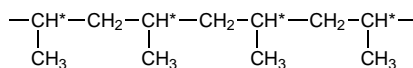


Figure 1. ^{13}C MAS NMR spectra (^1H decoupling only) of Ga-offretite with 50 Torr of adsorbed CH_3OH and heated at $300\text{ }^\circ\text{C}$ for (a) 10 min, (b) 2 h, (c) 4 h, (d) 6 h, (e) 8 h, and (f) 11 h.

luted spectral peaks. At longer thermal treatments the intensity of the line from DME decreases simultaneously with the growth of resonances from aliphatic carbons (-10 to $+40$ ppm). When Ga-offretite is heated at $300\text{ }^\circ\text{C}$ for 10 min, a new line at ca. 59 ppm from gaseous ethanol (EtOH) appears (Figure 1a). Support for this assignment comes from the spectrum recorded without proton decoupling where the line from the methylene carbon is split into a triplet with $J_{\text{C-H}} \approx 144\text{ Hz}$,⁴¹ characteristic of the methylene group in ethanol (the three peaks at high chemical shifts in Figure 4b, two of them superimposed on other peaks). The fact that a spectrum can be obtained at all without proton decoupling indicates that the motion of the species responsible is relatively fast. Further support for this conclusion comes from the disappearance of this line when the spectrum is recorded with cross-polarization as a result of motional averaging of the dipolar interaction on which CP relies (Figure 4c). On the other hand, in the dipolar dephasing experiment the line disappears with $60\text{ }\mu\text{s}$ dephasing (Figure 4d), as expected for the methylene group.⁴⁴ Two new lines are found in the $40\text{--}70$ ppm region, corresponding to long-chain hydrocarbons.³⁵ The magnitude of the ^{13}C chemical shifts shows that the species responsible are highly branched. The line at 56.8 ppm was previously assigned to the quaternary (starred) carbon in



and the resonance at 46 ppm to the ternary (starred) carbons in



A comparison of the spectrum recorded with proton decoupling and the dipolar-dephased spectrum (curves a, d, and e of Figure 4) confirms the assignment of the line at 56.8 ppm but militates against the earlier assignment of the 46 ppm line. Alemany et al.⁴⁴ found that the intensity of the line from the CH (methine)

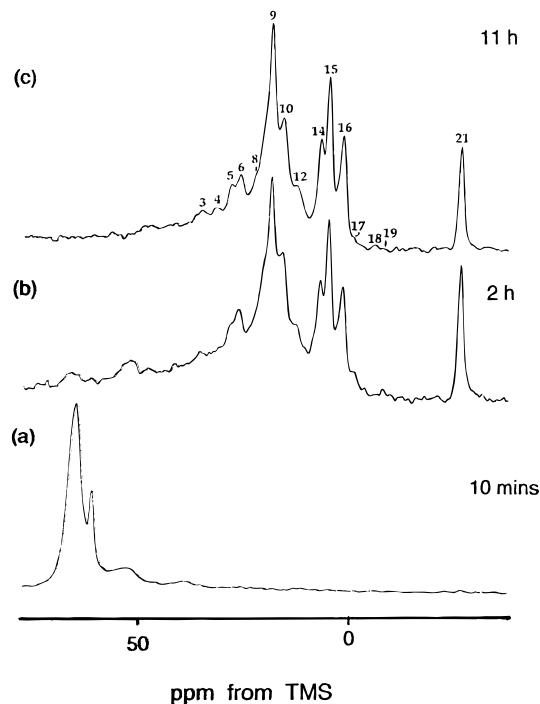


Figure 2. ^{13}C MAS NMR spectra (^1H decoupling only) of Al,Ga-offretite with 50 Torr of adsorbed CH_3OH heated at $300\text{ }^\circ\text{C}$ for (a) 10 min, (b) 2 h, and (c) 11 h.

group drops by ca. 75% at dephasing times of $25\text{--}55\text{ }\mu\text{s}$. However, the intensity of the line at 46 ppm did not decrease significantly at even longer dephasing times (up to $500\text{ }\mu\text{s}$) (Figure 4e). The origin of this line remains to be established.

Integration of deconvoluted NMR lines shows that the concentration of EtOH and highly branched compounds increases at $300\text{ }^\circ\text{C}$ for up to 11 h (Figure 1) and then decreases simultaneously with the growth of resonances from branched $\text{C}_4\text{--C}_5$ species. In Al,Ga-offretite (Figure 2) and Al-offretite (Figure 3), DME is no longer present after 2 and 3 h, respectively, showing that the conversion of MeOH to hydro-

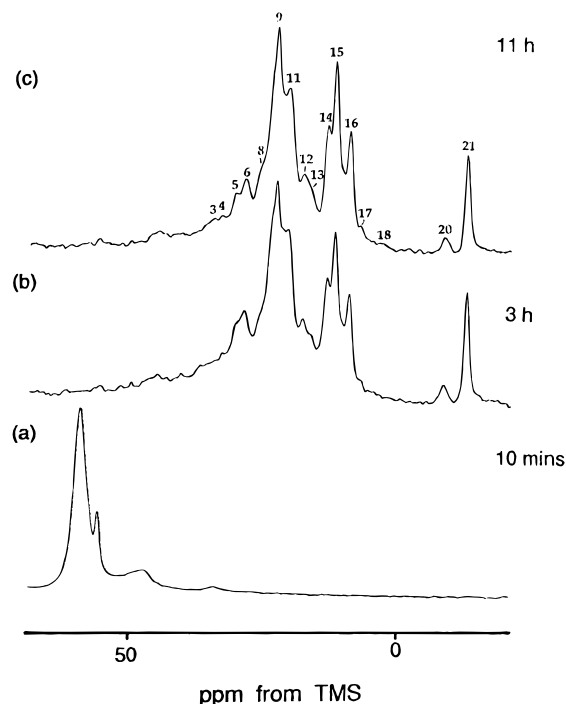


Figure 3. ^{13}C MAS NMR spectra (^1H decoupling only) of Al-offretite with 50 Torr of adsorbed CH_3OH heated at $300\text{ }^\circ\text{C}$ for (a) 10 min, (b) 3 h, and (c) 11 h.

carbons is complete. Complete conversion does not occur on Ga-offretite below $300\text{ }^\circ\text{C}$ (Figure 1) even after 11 h but is achieved after 10 min at $370\text{ }^\circ\text{C}$ when the lines from DME and EtOH disappear. The lines due to highly branched hydrocarbons are still visible, although their intensities decrease markedly with time.

The aliphatic region of the spectra of samples heated at $370\text{ }^\circ\text{C}$ (Figure 5) exhibits many of the lines already seen at $300\text{ }^\circ\text{C}$. The concentration of branched alkanes such as 3-methyl-

pentane, 2,3-dimethylbutane, and 3,3-dimethylpentane increases while that of straight-chain alkanes decreases.

The final product distribution for each sample is summarized in Table 3. The most striking difference among the three catalysts is that Ga-offretite gives a high concentration of highly branched hydrocarbons heavier than C_4 . On the other hand, considerably more methane and propane is produced with Al-offretite and Al,Ga-offretite than with Ga-offretite. Treatment at $370\text{ }^\circ\text{C}$ produces a number of very low-intensity resonances in the aromatic region (not shown). Since these lines are so weak and poorly resolved, their assignment is very difficult and not crucial.

Discussion

After treatment at $300\text{ }^\circ\text{C}$ for 10 min DME is still the only carbonaceous species formed. Hydrocarbons appear at longer reaction times while the concentration of DME decreases. An induction period is required for hydrocarbons to appear, and their formation is the rate-determining step in the MTG process.⁴⁵ No carbon monoxide^{14,29} or other oxonium compounds⁴⁶ are found at any temperature.

With Ga-offretite alone, EtOH appears before the formation of hydrocarbons begins and disappears upon complete conversion, indicating that EtOH is an intermediate in this sample.¹⁴ Although dehydration of ethanol yields ethylene, we have not found significant amounts of olefins, such as ethylene or propylene, at any stage of the reaction. Since the production of olefins is only favored at very high space velocities, when there is insufficient time for hydrogenation to occur,⁴⁷ one may expect that under static conditions, such as those used in our experiments, little or no olefins will be formed.³⁰

After treatment for 3 h at $300\text{ }^\circ\text{C}$, MeOH and DME in Al,Ga-offretite and Al-offretite are completely converted to a mixture of aliphatic compounds, but the equilibrium distribution of aliphatics is not established until the samples are treated at $370\text{ }^\circ\text{C}$ for 4 and 8 h, respectively. By contrast, in Ga-offretite

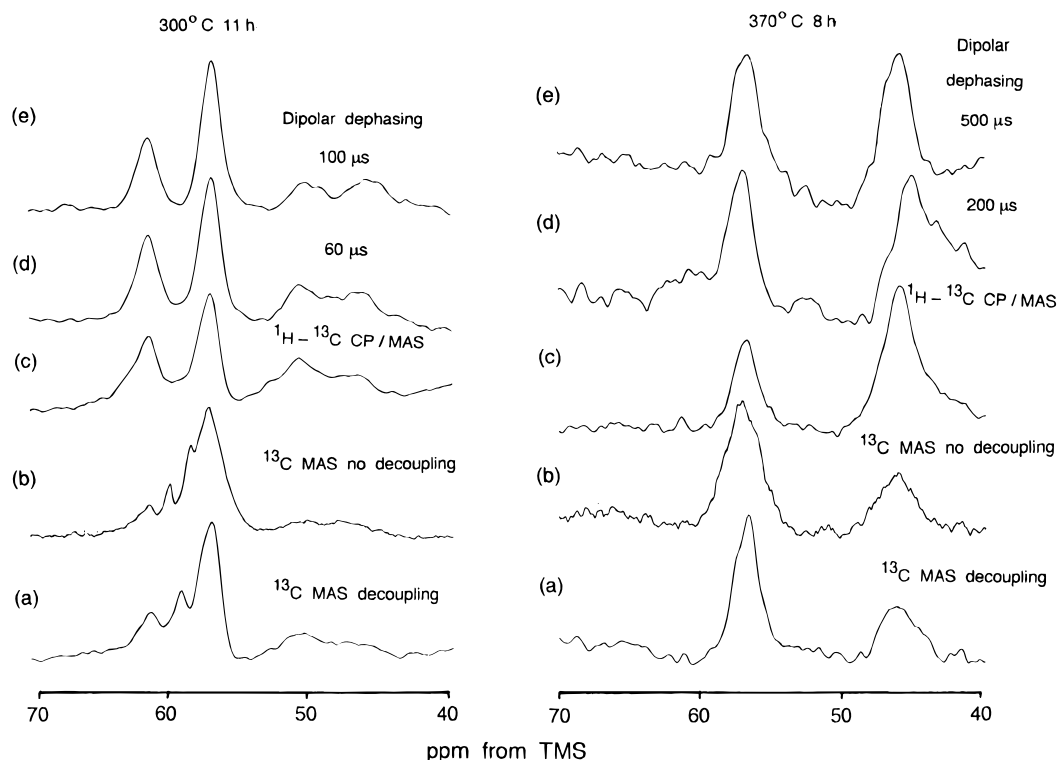


Figure 4. MAS NMR spectra of Ga-offretite with 50 Torr of adsorbed CH_3OH and heated at $300\text{ }^\circ\text{C}$ for 11 h and at $370\text{ }^\circ\text{C}$ for 8 h: (a) ^{13}C MAS with proton decoupling only; (b) ^{13}C MAS without proton decoupling; (c) ^1H - ^{13}C CP/MAS; (d) and (e) ^1H - ^{13}C dipolar dephasing.

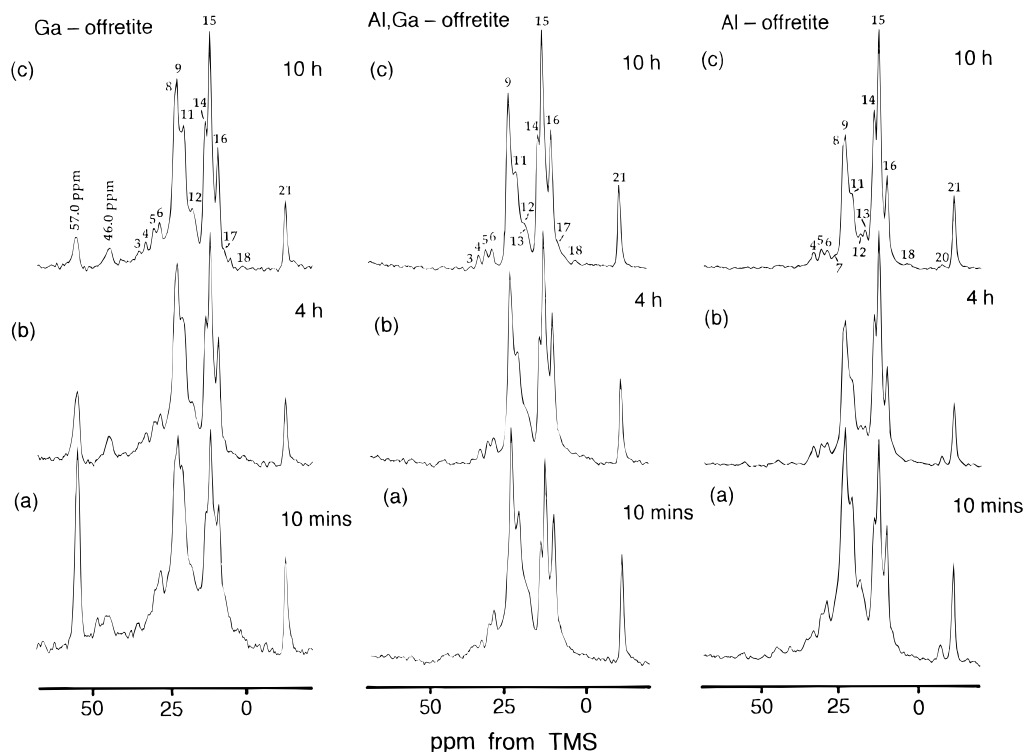


Figure 5. ^{13}C MAS NMR spectra (^1H decoupling only) of Ga-offretite, Al,Ga-offretite, and Al-offretite with 50 Torr of adsorbed CH_3OH heated at 370°C for (a) 10 min, (b) 4 h, and (c) 10 h.

the conversion of MeOH and DME into aliphatics requires treatment at 370°C for 10 min, but the equilibrium distribution of aliphatics is reached after 11 h at this temperature.

After treatment of Ga-offretite for 10 min at 300°C , branched long-chain hydrocarbons begin to form in the intracrystalline space but are unable to exit even at a temperature as high as 370°C and 14 h of treatment. We did not find such hydrocarbons in Al,Ga- and Al-offretites. However, the different behavior of Ga-offretite cannot be simply interpreted in terms of the microporous volume, since the volume of Ga-offretite is 50% lower than that of Al-offretite. Thus, crystallographic pore dimensions are not a simple guide to product selectivity. On the other hand, the lower reaction rate over Ga-offretite⁴⁰ enables us to monitor the intermediates absent from the other samples, where they immediately become involved in further reactions. As expected, the decreasing concentration of branched long-chain hydrocarbons with increasing temperature and time of treatment is accompanied by an increased concentration of branched low alkanes, their cracking products.⁴⁸ The distribution of the final products indicates the following.

(1) As the aluminum content of the catalyst increases, the concentration of straight-chain $\text{C}_4\text{--C}_7$ alkanes decreases and that of $\text{C}_1\text{--C}_3$ hydrocarbons increases. We note that cyclopropane is uniquely present in Al-offretite so that higher Brønsted acidity favors the cracking of long-chain hydrocarbons.

(2) As the gallium content of the catalyst increases, the concentration of $\text{C}_1\text{--C}_3$, the cracking products, falls but that of branched alkanes, such as 3-methylbutane and 2,3-dimethylbutane, increases. This, together with the presence of EtOH as a likely intermediate, indicates that dehydration/hydration on the Lewis sites does occur. This is compatible with the high Lewis acidity of Ga-offretite as determined by microcalorimetric measurements of the desorption of ammonia.

The mechanism of conversion of MeOH into gasoline is still controversial. It appears that at least two mechanisms, involving both Brønsted and Lewis acid sites, are at work. As monitored by NMR, extraframework Al and Ga species are generated

during the preparation of the hydrogen forms, giving rise to Lewis acid sites. On the other hand, adjacent hydroxyl groups condense at high temperatures to produce water and to generate accessible Al^{3+} or Ga^{3+} Lewis acid sites as well as O^{2-} Lewis basic sites, both known to be highly active for the dehydrogenation of alcohols and isomerization of alkenes.⁴⁹ The MTG process is thus bifunctional and involves Brønsted acid sites as well as extraframework Ga and Al species.

The yield of methane has been calculated by comparison of the intensity of the ^{13}C NMR line from methane under a given set of conditions with the intensity of the line from methanol adsorbed at room temperature. More methane is formed over the aluminum-containing samples, $3.2 \pm 0.1\%$ in Al-offretite and $3.7 \pm 0.1\%$ in Al,Ga-offretite, than in Ga-offretite ($2.0 \pm 0.1\%$). The presence of significant amounts of methane in some experiments is symptomatic of coke deposition,⁴⁸ indicating that the rate of coke formation increases with the density of acid sites and that extraframework gallium species are active hydrogenation catalysts that reduce coking.⁵⁰ To optimize the useful life of a catalyst, suitable concentrations of acid sites and extraframework gallium are required. However, by contrast with earlier reports,^{50,51} we have found that extraframework Ga does not promote aromatization.

Acknowledgment. We are grateful to the European Community for grants to M.D.A. and A.A.R., to Dr. H. He for experimental assistance, and to the Departamento de Química Orgánica, Universidad de Córdoba, for enabling us to perform the nitrogen adsorption measurements.

References and Notes

- (1) Cheng, C. F.; Klinowski, J. *J. Chem. Soc., Faraday Trans.* **1996**, 92, 289.
- (2) Cheng, C. F.; Alba, M. D.; Klinowski, J. *Chem. Phys. Lett.* **1996**, 250, 328.
- (3) Luan, Z. H.; Cheng, C. F.; Zhou, W. Z.; Klinowski, J. *J. Phys. Chem.* **1995**, 99, 1018.

- (4) Mokaya, R.; Jones, W.; Luan, Z. H.; Alba, M. D.; Klinowski, J. *Catal. Lett.* **1996**, 37, 113.
- (5) Liu, S. X.; He, H. Y.; Luan, Z. H.; Klinowski, J. *J. Chem. Soc., Faraday Trans.* **1996**, 92, 2011.
- (6) Chu, C. T. W.; Chang, C. D. *J. Phys. Chem.* **1985**, 89, 1569.
- (7) Chu, C. T. W.; Kuhl, G. H.; Lago, R. M.; Chang, C. D. *J. Catal.* **1985**, 93, 451.
- (8) Szostak, R.; Nair, V.; Thomas, T. L. *J. Chem. Soc., Faraday Trans. I* **1987**, 83, 487.
- (9) Simmons, D. K.; Szostak, R.; Agrawal, P. K.; Thomas, T. L. *J. Catal.* **1987**, 106, 287.
- (10) Gnep, N. S.; Doyemet, J. Y.; Seco, A. M.; Ribero, F. R. *Appl. Catal.* **1988**, 43, 155.
- (11) Kanai, J.; Kawata, N. *J. Catal.* **1988**, 114, 284.
- (12) Gnep, N. S.; Doyemet, J. Y.; Guisnet, M. *J. Mol. Catal.* **1988**, 45, 281.
- (13) Tsiao, C.; Corbin, D. R.; Dybowski, C. *J. Am. Chem. Soc.* **1990**, 112, 7140.
- (14) Anderson, M. W.; Klinowski, J. *Nature* **1989**, 339, 200.
- (15) Klinowski, J.; Anderson, M. W. *J. Magn. Reson.* **1990**, 28, S68.
- (16) Pope, C. G. *J. Chem. Soc., Faraday Trans.* **1993**, 89, 1139.
- (17) Bosáček, V. *J. Phys. Chem.* **1993**, 97, 10732.
- (18) Vetrivel, R.; Catlow, C. R. A.; Colbourn, E. A. *J. Phys. Chem.* **1989**, 93, 4594.
- (19) Gale, J. D.; Catlow, C. R. A.; Cheetham, A. K. *J. Chem. Soc., Chem. Commun.* **1991**, 178.
- (20) Haase, F.; Sauer, J. *J. Phys. Chem.* **1994**, 98, 3083.
- (21) Sauer, U.; Ugliengo, P.; Garrone, E.; Saunders, R. V. *Chem. Rev.* **1994**, 94, 2095.
- (22) Gale, J. D.; Catlow, C. R. A.; Carruthers, J. R. *Chem. Phys. Lett.* **1993**, 216, 155.
- (23) Csicsery, S. M. *Zeolites* **1984**, 4, 202.
- (24) Chen, N. Y.; Garwood, W. E. *Catal. Rev. Sci. Eng.* **1986**, 28, 185.
- (25) Derouane, E. G.; Vardendeken, D. *Appl. Catal.* **1988**, 45, 15.
- (26) Fraenkel, D.; Levy, M. *J. Catal.* **1989**, 119, 108.
- (27) Murray, D. K.; Chang, J. W.; Haw, J. F. *J. Am. Chem. Soc.* **1993**, 115, 4732.
- (28) Mirth, G.; Lercher, J. A.; Anderson, M. W.; Klinowski, J. *J. Chem. Soc., Faraday Trans.* **1990**, 86, 3039.
- (29) Anderson, M. W.; Klinowski, J. *J. Am. Chem. Soc.* **1990**, 112, 10.
- (30) Anderson, M. W.; Sulikowski, B.; Barrie, P. J.; Klinowski, J. *J. Phys. Chem.* **1990**, 94, 2730.
- (31) Anderson, M. W.; Klinowski, J. *J. Chem. Soc., Chem. Commun.* **1990**, 918.
- (32) Anderson, M. W.; Klinowski, J. *Chem. Phys. Lett.* **1990**, 172, 275.
- (33) Anderson, M. W.; Barrie, P. J.; Klinowski, J. *J. Phys. Chem.* **1991**, 95, 235.
- (34) Occelli, M. L.; Innes, R. A.; Pollack, S. S.; Sanders, J. V. *Zeolites* **1987**, 7, 265.
- (35) Anderson, M. W.; Occelli, M. L.; Klinowski, J. *J. Phys. Chem.* **1992**, 96, 388.
- (36) Cavalcante, C. L.; Eic, M.; Ruthven, D. M.; Occelli, M. L. *Zeolites* **1995**, 15, 293.
- (37) Occelli, M. L.; Innes, R. A.; Pollack, S. S.; Sanders, J. V. *Zeolites* **1987**, 7, 265.
- (38) (a) Alba, M. D.; Alvero, R.; Castro, M. A.; Trillo, J. M. *Multifunctional Mesoporous Inorganic Solids. Series C*; Kluwer Academic Publishers: London, 1993; Vol. 400, p 49. (b) Trillo, J. M.; Alba, M. D.; Castro, M. A.; Poyato, J.; Tobías, M. M. *J. Mater. Sci.* **1993**, 28, 373.
- (39) Carpenter, T. A.; Klinowski, J.; Tennakoon, D. T. B.; Smith, C. J.; Edwards, D. C. *J. Magn. Reson.* **1986**, 68, 561.
- (40) Alba, M. D.; Romero, A. A.; Occelli, M. L.; Klinowski, J. *J. Chem. Soc., Faraday Trans.* **1997**, 93, 1221.
- (41) Pertsch, E.; Simon, W.; Seibl, J.; Clerc, T. *Tables of Spectral Data for Structure Determination of Organic Compounds*; Springer-Verlag: Berlin, 1989.
- (42) Engelhardt, G.; Michel, D. *High-Resolution Solid-State NMR of Silicates and Zeolites*; Wiley: Chichester, 1987.
- (43) Xu, Y.; Grey, C. P.; Thomas, J. M.; Cheetham, A. K. *Catal. Lett.* **1990**, 4, 251.
- (44) Alemany, L. B.; Grant, D. M.; Alger, T. D.; Pugmire, R. J. *J. Am. Chem. Soc.* **1983**, 105, 6697.
- (45) (a) Ouo, Y.; Mori, T. *J. Chem. Soc., Faraday Trans. I* **1981**, 77, 2209. (b) Chen, N. Y.; Reagan, W. J. *J. Catal.* **1979**, 59, 123.
- (46) Jackson, J. E.; Bertsch, F. M. *J. Am. Chem. Soc.* **1990**, 112, 9085.
- (47) Chang, C. D.; Silvestri, A. J. *J. Catal.* **1977**, 47, 249.
- (48) Chang, C. D. *Hydrocarbons from Methanol*; Marcel Dekker: New York, 1983.
- (49) Atkins, P. W. *Physical Chemistry*; Oxford University Press: 1994; p 560.
- (50) Kanai, J.; Kawata, N. *Appl. Catal.* **1990**, 62, 141.
- (51) (a) Kitagawa, H.; Sendoda, Y.; Ono, Y. *J. Catal.* **1986**, 101, 12. (b) Meriaudeau, P.; Naccache, C. *J. Mol. Catal.* **1989**, 50, L7.